https://doi.org/10.1016/j.trc.2021.103190

Dynamic user equilibrium for departure time choice in the basic trip-based model

R. X. ZHONG[1] [a], J. H. XIONG[1] [b], Y. P. HUANG [c], N. ZHENG [d], William H.K. LAM [c], T. L. PAN [e,*], B. HE [e,*]

[a] *School of Intelligent Systems Engineering, Sun Yat-Sen University, Guangzhou, China.*
[b] *Guangzhou Transport Planning Research Institute, Guangzhou, China*
[c] *Department of Civil and Environmental Engineering, The Hong Kong Polytechnic University, Hong Kong SAR, China*
[d] *Institute of Transport Studies, Department of Civil Engineering, Monash University, Australia*
[e] *Research Institute of Smart City, Shenzhen University, Shenzhen, China.*

Abstract

Recent research indicates that the trip-based models can perform more accurately for capturing network hyper-congestion than the conventional macroscopic fundamental diagram (MFD) dynamics, especially during transient phases. However, due to the complex mathematical structure of the trip-based models, deriving analytical properties of the dynamic user equilibrium (DUE) of departure time choice with the trip-based models is still a challenge. This paper investigates the DUE problem of departure time choice in an isotropic urban network with identical travelers. Traffic dynamics is captured by the basic trip-based model using a speed-MFD that maps the traffic accumulation to the space-mean speed of the network. Necessary conditions for dynamic user equilibrium with and without inflow capacity constraint are derived, respectively. Under dynamic user equilibrium condition, no traveler can reduce her/his travel cost by changing the departure time. The analysis reveals the significant difference between the basic trip-based model and the conventional MFD models regarding the information support involved in the departure time choice. The derivation does not rely on some common assumptions in the literature such as linear travel cost function, no late arrivals, or linear speed-MFD. The numerical example indicates that the inflow capacity constraint can help prevent two peaks in the departure profile and the vehicle accumulation.

Keywords: Macroscopic fundamental diagram, trip-based model, departure time choice, dynamic user equilibrium, scheduling preference.

1. Introduction

The bottleneck model introduced by Vickrey (1969) has been widely employed to study the rush-hour traffic congestion and the subsequent equilibrium behavior. Due to its point queue assumption, Vickrey's

[1] These authors contributed equally to this work.

[*] Corresponding author.
E-mail addresses: zhrenxin@mail.sysu.edu.cn (R. X. ZHONG)., xiongjh3@mail2.sysu.edu.cn (J. H. XIONG)., yunping.huang@connect.polyu.hk (Y. P. HUANG)., Nan.Zheng@monash.edu (N. ZHENG)., william.lam@polyu.edu.hk (William H.K. LAM)., glorious9009@gmail.com (T. L. PAN)., 1688698@qq.com (B. HE).

bottleneck model and its extensions are analytically tractable. However, as pointed out in Arnott (2013); Arnott et al. (2016); Arnott and Buli (2018), Vickrey's bottleneck cannot capture the hyper-congestion. Li and Huang (2017, 2018) adopted the LWR model and the Greenshields' relation to describe the traffic dynamics of a single-entry freeway corridor and to derive the user equilibrium (UE) and/or social optimum (SO) conditions. However, congestion of urban networks cannot be modeled as collections of independent (point) bottlenecks. Recently, the seminal papers by Daganzo (2007); Daganzo and Geroliminis (2008); Geroliminis and Daganzo (2008) proposed a network-scale macroscopic fundamental diagram (MFD) to capture the effect of hyper-congestion on the network level. The MFD establishes an equilibrium relationship between network traffic accumulation and network outflow. In conjunction with the law of flow conservation, the MFD describes the network traffic flow evolution based on several assumptions such as homogeneously distributed traffic congestion and stationary travel demand. A fascinating property of the MFD dynamics is that it is analytically tractable (Daganzo and Geroliminis, 2008; Buisson and Ladier, 2009; Geroliminis and Sun, 2011; Saberi et al., 2014; Zhong et al., 2018a,b). Small and Chu (2003) applied the MFD dynamics to investigate the departure time choice by emphasizing the cost of hyper-congestion.

To enable departure time choice, we need to properly define the travel time with respect to the time-varying traffic condition. In the literature, there are mainly two approaches for evaluating the network travel time. The first approach assumes that the outflow function of the conventional accumulation-based MFD model (without modeling the travel time function in the flow propagation explicitly), see Mariotte et al. (2017) or the travel time of the accumulation-based MFD model with time delay (modeling the travel time function in the flow propagation explicitly), see Small and Chu (2003); Huang et al. (2020), is determined by the network traffic conditions at the instant of entering the network. Conventionally, the average network travel time function at time t is a function of the network accumulation $n(t)$ at time t, i.e.,

$$h(n(t)) = \frac{n(t)}{\mathcal{G}(n(t))} \tag{1}$$

where $\mathcal{G}(n(t))$ is the (outflow) MFD of the network. Such approach is widely used in the perimeter and gating traffic control based on the MFD framework, e.g., Keyvan-Ekbatani et al. (2012); Haddad and Mirkin (2016); Mirkin et al. (2016); Haddad and Zheng (2020), and the region-level route guidance or departure time choice, e.g., Small and Chu (2003); Yildirimoglu and Geroliminis (2014); Yildirimoglu et al. (2015, 2018); Aghamohammadi and Laval (2020); Ni and Cassidy (2020).

On the other hand, the second approach assumes that travel time depends on the time-varying traffic speed over the course of a trip. In this approach, the travel time is evaluated by the integral of duration over each distance increment of his/her trip (Arnott, 2013; Fosgerau, 2015; Arnott et al., 2016; Lamotte and Geroliminis, 2018; Mariotte et al., 2017; Arnott and Buli, 2018; Mariotte and Leclercq, 2019). Mathematically, travel time $h(t)$ as a function of departure time t is given implicitly by

$$\int_{t}^{t+h(t)} v(n(s))ds = L \tag{2}$$

where L is the distance travelled, $v(n(s))$ is the average network traffic speed at time s when the network accumulation is $n(s)$. This formulation aims at modeling the impact of the time-varying traffic speed $v(n(s))$ within a trip duration and the trip length L on the travel time function $h(t)$. If the trip length is assumed to be uniform, the MFD with such a travel time function is termed as the (basic) trip-based (or bathtub) model (Arnott and Buli, 2018).

Recent research indicates that the trip-based model can perform more accurately in capturing network hyper-congestion than the conventional accumulation-based MFD dynamics, especially during transient

phases. This is because the travel time function is explicitly incorporated in the flow propagation in the trip-based model, see Mariotte et al. (2017); Paipuri and Leclercq (2020). However, every coin has two sides, incorporating the travel time function in the flow propagation also renders the trip-based dynamics become delay differential equations (DDEs). The DDE introduces a serious weakness to the trip-based MFD dynamics that the solution of the equilibria and optima is generally analytically intractable (Arnott and Buli, 2018).

Under the assumption of homogeneous users, Fosgerau and Small (2013); Arnott (2013) found that the benefits of congestion pricing using MFD the network loading model could be even greater than that with Vickrey's bottleneck model if the pricing scheme can maintain the system at the flow-maximizing accumulation. Arnott et al. (2016) derived a closed-form solution of an equilibrium when no late arrivals are permitted for a special case of the bathtub model with $\alpha - \beta - \gamma$ form of the cost function. Several assumptions such as identical commuters, a trip cost function that is linear in travel time and schedule delay, no late arrivals, and the average network velocity is a negative linear function of traffic density are imposed. Combining Vickrey's bottleneck model with the MFD, Amirgholy and Gao (2017) developed a bathtub model for approximating the user equilibrium of the morning commute problem under several assumptions, e.g., the equilibrium trajectory can be well approximated by a quadratic function. Arnott and Buli (2018) further pursued numerical solution algorithm to the equilibrium with the basic bathtub model under the assumption that the utility or trip cost function is a smooth function of its arguments while following the same linear speed-density relationship in line with Arnott et al. (2016). Li and Huang (2019) extended the basic trip-based model to consider the continuous schedule preference. Based on the assumption that the velocity-density function and the schedule delay penalty function are linear, the user equilibrium and system optimum with continuous departure rate were derived. All the above references consider an isotropic downtown area with identical commuters in terms of trip length. Recognizing the trip length heterogeneity would challenge the fundamental FIFO assumption, Fosgerau (2015); Daganzo and Lehe (2015) investigated the impacts of trip length heterogeneity on the morning commute while reaching very different conclusions on the role of trip length. The differences are possibly due to the different scheduling preferences chosen and the underlying simplified traffic dynamics. Assuming exponential-type scheduling preferences, Fosgerau (2015) showed that two users differing by their trip lengths sort according to a Last-In, First-Out (LIFO) pattern under user equilibrium wherein the user with the longest trip starts earlier and finishes later. On the other hand, using conventional $\alpha - \beta - \gamma$ scheduling preferences, Daganzo and Lehe (2015) proved that the social optimum persists the First-In-First-Out (FIFO) property under a simplified congestion mechanism similar to the point bottleneck model. They further concluded that the FIFO is strict only within families of users having identical scheduling preferences and heterogeneous trip lengths. Arnott and Buli (2018); Lamotte and Geroliminis (2018); Aghamohammadi and Laval (2020) encouraged further research effort to the determination of necessary and sufficient conditions for dynamic traffic equilibria including user equilibrium and system optimum.

This paper investigates the dynamic user equilibrium for departure time choice in the basic trip-based model. Parallel to the numerical treatments developed in the literature, we focus on deriving the analytical dynamic user equilibrium condition under general travel time function and schedule penalty function. Inflow capacity constraint is imposed to restrict the departure rate from exceeding the network capacity. The analysis reveals the significant difference between the basic trip-based model and the conventional MFD models regarding the information support involved in the departure time choice. We show numerically that the inflow capacity constraint with a proper width of the desired departure time window can avoid the phenomenon of two peaks in the departure profile and the vehicle accumulation, which is considered as an undesired property by Lamotte and Geroliminis (2018).

Paper organization: Section 2 introduces the basic trip-based model for network representation and several common assumptions. Section 3 formulates the departure time choice problem for the basic trip-based model and derives the necessary conditions of the equilibrium conditions through the lens of Pontryagin minimum principle. Numerical examples are worked out to illustrate the properties of the DUE in Section 4 based on the numerical algorithm outlined in Appendix A. Finally, Section 5 concludes the paper. Companion materials are presented in the appendix.

2. The basic trip-based model

To begin with, we summarize the nomenclature used in this paper in Table 1.

Table 1: Nomenclature

Q	Travel demand of the region
$q(t)$	Departure rate at time t with $q_{\max}$ as the upper bound
$G(t)$	Trip completion rate at time t
$n(t)$	Traffic accumulation of the region at time t
$v(t)$	Average traffic speed of the region at time t
$\mathcal{V}(n)$	Speed-MFD of the region
$h(\cdot)$	Theorectical travel time of the region (Forward in time)
$\sigma(\cdot)$	Experienced travel time of the region (Backward in time)
$\Psi(\cdot)$	Total travel cost including the schedule delay penalty
ϕ	Minimum travel cost
MFD	Macroscopic fundamental diagram
DUE	Dynamic user equilibrium
FIFO	First-In-First-Out

In line with Arnott and Buli (2018), we impose the following assumptions:

Assumption 2.1. In the basic trip-based model, it is assumed that a fixed number of commuters travel an equal distance L from home to work over an isotropic downtown area during the morning rush hour. All travelers have identical scheduling preference.

Assumption 2.2. At any time instant, the average traffic velocity depends on the network traffic accumulation (or density) at that time. The speed-MFD function $\mathcal{V}(n)$ is assumed to be positive, continuously differentiable and strictly decreasing on the interval $[0, n_{jam}]$, i.e., from empty to gridlock. The free-flow speed $\mathcal{V}(n = 0)$ is denoted as v_f.

In Arnott and Buli (2018), $v(k) = v_f\left(1 - \frac{k}{k_j}\right)$, a linear relation (i.e., Greenshields) between velocity and density is assumed to simplify the problem.

Assumption 2.3. The utility or trip cost function is a smooth function of its arguments.

Following Lamotte and Geroliminis (2018); Arnott and Buli (2018), the FIFO condition will be guaranteed by Assumption 2.1. Due to the FIFO, all vehicles entering the network at the same time, say t, would have the same travel time, say $h(t)$, and therefore exiting the network at the same time, say $t + h(t)$, as well. In this sense, we can define the travel time for a commuter departing at time t by subtracting the time when

the cumulative outflow equals to the cumulative inflow at the time he/she enters the network. In terms of flow conservation, this implies

$$\int_0^t q(s)\mathrm{d}s = \int_0^{t+h(t)} G(s)\mathrm{d}s \tag{3}$$

where $q(t)$ is the departure rate at time t and $G(t)$ is the trip completion (or outflow) rate at time t. Differentiating (2) and (3) yields

$$v\left(t+h(t)\right)\left(1+\dot{h}(t)\right) = v(t) \tag{4}$$

$$G\left(t+h(t)\right)\left(1+\dot{h}(t)\right) = q(t) \tag{5}$$

From the above equations, with $1+\dot{h}(t) > 0$ under the FIFO condition, we have the following relationship among the outflow, the network velocity, and the travel time

$$G(t+h(t)) = \frac{v(t+h(t))}{v(t)} q(t) \tag{6}$$

The evolution of network accumulation $n(t)$ can be defined as

$$\dot{n}(t) = q(t) - G(t) \tag{7}$$

At the end of the planning horizon, all the travel demand should be served, i.e.,

$$\int_0^T q(s)ds = Q \tag{8}$$

where Q is the total travel demand.

To distinguish "history (or memory)" and "future" states of the network, we further introduce the "experienced" (or inverse) travel time function $\sigma(t)$, which denotes the travel time of vehicles exiting the network at time t (i.e., exit time). Note that $h(t)$ is the travel time for vehicles entering the network at time t (i.e., entry time), the relationship between these two definitions of travel time as depicted in Figure 1 can be casted as

$$\sigma(t) = h\left(t-\sigma(t)\right)$$

Regarding t as "current" time, we have $\sigma(t)$ known (and thus experienced) and time $t-\sigma(t)$ as "history". Since $h(t)$ depends on the traffic speed throughout the trip duration, it is unknown and yet to be determined until the trip is completed. Therefore, we regard its exit time $s = t+h(t)$ as "future" (with respect to t). And we have the following domains for these time indexes:

$$t \in [0,T] \Longleftrightarrow s \in [h(0), T+h(T)]$$

As the network is empty at time T (i.e., all travel demand has been served), $\sigma(T)$ and $h(T)$ should be the free-flow time. We denote the free-flow time τ as

$$\sigma(n \to 0) = h(n \to 0) = \tau$$

From the definitions of vehicle accumulation and experienced travel time in the sense of flow conservation (as shown in Figure 1), we can see that the vehicle accumulation at a specific time t, i.e., $n(t) = N_{in}(t) - N_{out}(t)$, is a result of the historical inflow profile during $[t-\sigma(t),\ t]$, i.e., $n(t) = N_{in}(t) - N_{in}\left(t-\sigma(t)\right)$ noting

$N_{in}(t-\sigma(t)) = N_{out}(t)$. On the other hand, during the vehicles' presence in the network, their trip duration $h(t)$ is a result of the "future" network speed till they exit from the network by (2) (and also (3)). Therefore, we claim that the traffic state of trip-based models is determined by both the memory and the "future" of the network. This introduces significant difficulties in analyzing the equilibrium patterns with the trip-based models, see e.g., Arnott and Buli (2018).

Moreover, we have

$$t + h(t) - s = 0$$

Evaluating the derivative of the implicit function, we have

$$\frac{\mathrm{d}t}{\mathrm{d}s} = -\frac{\frac{\partial(t+h(t)-s)}{\partial s}}{\frac{\partial(t+h(t)-s)}{\partial t}} = \frac{1}{1+\dot{h}(t)} \Longrightarrow \mathrm{d}t = \frac{1}{1+\dot{h}(t)}\mathrm{d}s$$

Finally, the following relationship can be derived for these two definitions of travel time:

$$\frac{\mathrm{d}\sigma(s)}{\mathrm{d}s} = \frac{\mathrm{d}h\left(s-\sigma(s)\right)}{\mathrm{d}s} = \frac{\mathrm{d}h\left(s-\sigma(s)\right)}{\mathrm{d}\left(s-\sigma(s)\right)}\frac{\mathrm{d}\left(s-\sigma(s)\right)}{\mathrm{d}s} = \dot{h}\left(s-\sigma(s)\right)\left(1-\frac{\mathrm{d}\sigma(s)}{\mathrm{d}s}\right)$$

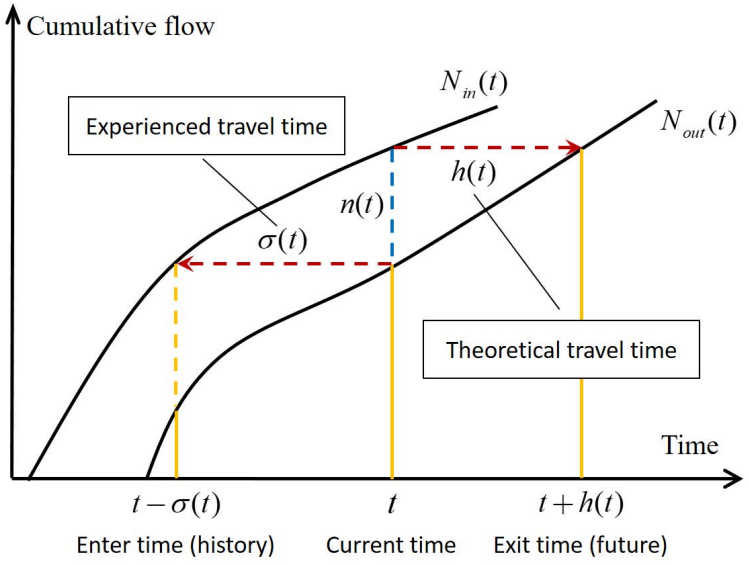

Figure 1: Relationship between time index and travel time

Several constraints should be imposed on the network outflow. Since vehicles can only depart during $[0, T]$, no vehicle should exit the network during $t \in [0, h(0)]$, i.e.,

$$G(t) = 0, t \in [0, h(0)]$$

On the other hand, all vehicles should exit the network before T. Therefore, $G(t) = 0,\ \forall t \geq T$. If we choose $s = t + h(t)$ (i.e., the exit time) as time index we must have

$$G(s) = 0, s \in [T, T + h(T)]$$

3. Dynamic user equilibrium analysis for departure time choice in the basic trip-based model

A schedule penalty function (or early/late arrival penalty), say $\kappa(\chi)$, is required to enable departure time choice. The schedule penalty function is usually chosen as a convex function. The total travel cost for a vehicle departing at time t is a summation of this penalty and the travel time, i.e.,

$$\Psi(t, v) = h(t) + \kappa(\chi) \tag{9}$$

where χ is the difference between actual arrival time and preferred arrival time t^*, $\chi = t + h(t) - t^*$, with $t^* < T$. According to Assumption 2.3, this function is a smooth function of its arguments.

Note that in the basic trip-based model, the travel time of a trip is a direct consequence of the dynamic network traffic speed, say equation (2). Therefore, we highlight this in the definition of total travel cost. Also note that the network accumulation is a direct consequence of the inflow to the region and is related with the inflow, outflow and traffic speed of the network through (6). Therefore, the control variables are chosen as the inflow rate $q(t)$ entering the network and the network traffic velocity $v(t)$ governed by the speed-MFD function $\mathcal{V}(n)$. Each commuter chooses her/his departure time to minimize her/his travel cost. Equilibrium is achieved when no commuter can decrease his/her travel cost by altering the departure time (Arnott and Buli, 2018). This is a special case of the dynamic user equilibrium with departure time choice, see e.g., Friesz and Han (2019). We formulate the departure time choice problem in the basic trip-based model by following the optimal control reformulation of the general DUE problem proposed in Friesz and Han (2019); Huang et al. (2020).

Definition 3.1. Dynamic user equilibrium (Friesz and Han, 2019). For any $\boldsymbol{q}^* \in \check{\Lambda}$ with

$$\check{\Lambda} = \left\{ \boldsymbol{q} : \boldsymbol{q}(t) \geq 0, \quad \int_0^T q^p(t)\,\mathrm{d}t = Q_w, \ \forall t \in [0, T] \right\}, \tag{10}$$

the vector of path flows as $\boldsymbol{q} = (q^p : p \in \mathcal{P})$ and any nonnegative vector $\boldsymbol{\phi} = (\phi_w : w \in \mathcal{W}) \in R_+^{|W|}$, the pair $(\boldsymbol{q}^*, \boldsymbol{\phi})$ is a simultaneous departure-time-and-route-choice dynamic user equilibrium if and only if the following two conditions are satisfied for all $p \in \mathcal{P}_w$ and for all $w \in \mathcal{W}$:

$$\begin{array}{rcccrcl} q^{p\,*}(t) & > & 0 & \Rightarrow & \Psi^p(t, \boldsymbol{q}^*) & = & \phi_w, \\ \Psi^p(t, \boldsymbol{q}^*) & > & \phi_w & \Rightarrow & q^{p\,*}(t) & = & 0, \end{array} \tag{11}$$

where ϕ_w is the smallest travel cost for the OD pair w given by

$$\phi_w = \min\{\varrho^p : p \in \mathcal{P}_w\} > 0, \ \forall w \in \mathcal{W}, \ \text{and} \ \varrho^p = \operatorname{ess\,inf}\{\Psi^p(t, \boldsymbol{q}) > 0 : t \in [0, \ T]\}, \ \forall p \in \mathcal{P}$$

where ess inf is essential infimum which defines the largest essential lower bound for a given function f wherein all $\inf f \leq \operatorname{ess\,inf} f$. ∎

Dynamic user equilibrium with departure time choice

$$\min \quad \int_0^T \Psi(v^*, t) q(t) dt$$

subject to

$$\frac{\mathrm{d}n(t)}{\mathrm{d}t} = q(t) - G(t), \qquad (\alpha(t)) \tag{12a}$$

$$v\left(t + h(t)\right) q(t) = v(t) G\left(t + h(t)\right), \qquad (\mu(t)) \tag{12b}$$

$$\frac{\mathrm{d}E(t)}{\mathrm{d}t} = q(t), \qquad (\rho(t)) \tag{12c}$$

$$E(T) = Q, \qquad (\phi) \tag{12d}$$

$$v(t) = \mathcal{V}(n(t)), \qquad (\xi(t)) \tag{12e}$$

$$-q(t) \leqslant 0, \qquad (\gamma(t)) \tag{12f}$$

$$q(t) - q_{max} \leqslant 0, \qquad (\zeta(t)) \tag{12g}$$

where $E(0) = 0$ and without loss of generality, we assume zero initial condition $n(0) = 0$. As explained in Section 2, (12a) and (12b) define network traffic dynamics and flow propagation constraint of the basic trip-based model, respectively. (12c) and (12d) define the travel demand. (12e) specifies the speed-MFD. (12f) is the nonnegative flow constraint. (12g) restricts that the inflow to the region should be less than its maximum service rate or capacity. Variables in brackets of (12a)-(12g) are Lagrange multipliers associated with the corresponding constraints, respectively.

Proposition 3.1. The necessary condition for departure time choice equilibrium of the basic trip-based model with inflow capacity constraint can be stated as:

$$q(t) \begin{cases} > 0, \Psi(v^*, t) + \zeta(t) = \phi \\ = 0, \Psi(v^*, t) + \zeta(t) > \phi \end{cases} \tag{13}$$

where ϕ is the equilibrium travel cost, $\zeta(t)$ is the additional cost caused by the traffic control via imposing an upper bound constraint on the inflow rate, and $\Psi(v^*, t)$ is the travel cost of the vehicles departing at time t. When there is no inflow capacity constraint, the equilibrium condition reduces to

$$q(t) \begin{cases} > 0, \Psi(v^*, t) = \phi \\ = 0, \Psi(v^*, t) > \phi \end{cases} \tag{14}$$

∎

Remark 3.1. Proposition 3.1 states that, for any time instant t, when the corresponding generalized travel cost equals to the user equilibrium cost, the departure rate $q(t) > 0$; otherwise, when the generalized cost exceeds the equilibrium, no travelers would depart. Comparing Proposition 3.1 with Definition 3.1, we can see that (14) is an equivalent expression of (11) when there is no inflow capacity constraints. In case of the inflow capacity constraints, as every constraint comes with a cost when it is violated, $\zeta(t)$ reflects the additional cost caused by the traffic control via imposing an upper bound constraint on the inflow rate, see (13). This can be regarded as an extension of the DUE case (Zhong et al., 2011; Huang et al., 2020).

Although the equilibrium condition in (14) seems simpler than that in (13), it does not necessarily imply (14) is easier to achieve than (13). We will discuss several possible reasons due to the "memory" effect of flow propagation and the prediction of "future" traffic state required by the basic trip-based model in Remark 3.2 and the numerical examples. ∎

Proof of Proposition 3.1. As claimed in Arnott and Buli (2018), given the speed-MFD function $\mathcal{V}(n)$, the basic trip-based model can be solved from the departure rate $q(t)$. Therefore, the objective is to solve for $q(t)$ that is consistent with the equilibrium condition. To derive the equilibrium condition, we define the Hamiltonian function for the optimal control problem as

$$\begin{aligned} H(q, G, n, v, E) =& \Psi(v^*, t)q(t) + \alpha(t)[q(t) - G(t)] + \rho(t)q(t) + \mu(t)\left[\tilde{v}(t)q(t) - v(t)\tilde{G}(t)\right] \\ &+ \xi(t)[v(t) - \mathcal{V}(n(t))] - \gamma(t)q(t) + \zeta(t)\left(q(t) - q_{max}\right) \end{aligned}$$

where we have used

$$\tilde{G}(t) = G(t + h(t)) = G(s), \qquad \tilde{v}(t) = v\left(t + h(t)\right) = v(s)$$

to save notation.

Applying the Pontryagin Minimum Principle, we have

$$\frac{\partial H}{\partial q(t)} = \Psi(v^*, t) + \alpha(t) + \rho(t) + \mu(t)\tilde{v}(t) - \gamma(t) + \zeta(t) \tag{15a}$$

$$\frac{\partial H}{\partial G(t)} = -\alpha(t) \tag{15b}$$

$$\frac{\partial H}{\partial \tilde{G}(t)} = -\mu(t)v(t) \tag{15c}$$

$$\frac{\partial H}{\partial n(t)} = -\xi(t)\frac{\partial \mathcal{V}(n(t))}{\partial n(t)} \tag{15d}$$

$$\frac{\partial H}{\partial v(t)} = -\mu(t)\tilde{G}(t) + \xi(t) \tag{15e}$$

$$\frac{\partial H}{\partial \tilde{v}(t)} = \mu(t)q(t) \tag{15f}$$

$$\frac{\partial H}{\partial E(t)} = 0 \tag{15g}$$

and the following stationary condition regarding the departure rate $q(t)$

$$\frac{\partial H}{\partial q(t)} = 0, t \in [0, T] \tag{16}$$

A set of costate equations:

$$\frac{\mathrm{d}\alpha(t)}{\mathrm{d}t} = -\frac{\partial H}{\partial n(t)}, t \in [0, T] \tag{17a}$$

$$\frac{\mathrm{d}\rho(t)}{\mathrm{d}t} = -\frac{\partial H}{\partial E(t)}, t \in [0, T] \tag{17b}$$

And the boundary condition

$$-\rho(T) - \phi = 0 \tag{18}$$

As discussed in Section 2, some variables, such as $G(t)$ and $\tilde{G}(t)$; $v(t)$ and $\tilde{v}(t)$, are not independent but related through flow propagation constraints. Therefore, we need to sort out how their dependence would affect the

optimality (stationary) condition. To see this, we evaluate the variation of the Hamiltonian function with respect to $G(t)$ and $\tilde{G}(t)$ as

$$\delta_{H_G} = \int_0^T \left[\frac{\partial H}{\partial G}\delta G + \frac{\partial H}{\partial \tilde{G}}\delta\tilde{G}\right]\mathrm{d}t = \int_0^T \frac{\partial H}{\partial G(t)}\delta G(t)\mathrm{d}t + \int_0^T \frac{\partial H}{\partial \tilde{G}(t)}\delta\tilde{G}(t)\mathrm{d}t$$
$$= \int_0^T \frac{\partial H}{\partial G(t)}\delta G(t)\mathrm{d}t + \int_0^T \frac{\partial H}{\partial \tilde{G}(t)}\delta G\left(t+h(t)\right)\mathrm{d}t$$

Note that

$$s = t + h(t)$$
$$t = 0, s = h(0); t = T, s = T + h(T)$$
$$\mathrm{d}t = \left[\frac{1}{1+\dot{h}(t)}\right]_{t=s-\sigma(s)} \mathrm{d}s$$
$$\tilde{G}(t) = G(t + h(t)) = G(s)$$

We have

$$\delta_{H_G} = \int_0^T \frac{\partial H}{\partial G(t)}\delta G(t)\mathrm{d}t + \int_{h(0)}^{T+h(T)} \left[\frac{\partial H}{\partial \tilde{G}(t)}\frac{1}{1+\dot{h}(t)}\right]_{t=s-\sigma(s)} \delta G(s)\mathrm{d}s$$
$$= \int_0^{h(0)} \frac{\partial H}{\partial G(t)}\delta G(t)\mathrm{d}t + \int_T^{T+h(T)} \left[\frac{\partial H}{\partial \tilde{G}(t)}\frac{1}{1+\dot{h}(t)}\right]_{t=s-\sigma(s)} \delta G(s)\mathrm{d}s$$
$$+ \int_{h(0)}^T \frac{\partial H}{\partial G(t)}\delta G(t)\mathrm{d}t + \int_{h(0)}^T \left[\frac{\partial H}{\partial \tilde{G}(t)}\frac{1}{1+\dot{h}(t)}\right]_{t=s-\sigma(s)} \delta G(s)\mathrm{d}s$$

We unify the time variables in the integral by $\theta \in [0, T + h(T)]$ and have in mind that G **is evaluated by the entry time** t **while** $\tilde{G}$ **is evaluated by the exit time** s**.** It follows:

$$\delta_{H_G} = \int_0^{h(0)} \frac{\partial H}{\partial G(\theta)}\delta G(\theta)\mathrm{d}\theta + \int_T^{T+h(T)} \left[\frac{\partial H}{\partial \tilde{G}(\theta)}\frac{1}{1+\dot{h}(\theta)}\right]_{t=\theta-\sigma(\theta)} \delta G(\theta)\mathrm{d}\theta$$
$$+ \int_{h(0)}^T \left\{\frac{\partial H}{\partial G(\theta)} + \left[\frac{\partial H}{\partial \tilde{G}(t)}\frac{1}{1+\dot{h}(t)}\right]_{t=\theta-\sigma(\theta)}\right\}\delta G(\theta)\mathrm{d}\theta$$

In the above equation, we regard θ as the current time. For vehicles exiting the network at time θ, they should enter the network at time $\theta - \sigma(\theta)$. Therefore, a physical interpretation to the above equation is that we trace the memory (i.e., "history") of the network to the entry time of the flow exiting the network at time θ to deduce the effect of this amount of flow on the equilibrium condition (see also the "memory" effect of flow propagation explained on Pages 5-6 and depicted in Figure 1 in Section 2). Thus, we obtain

$$\frac{\partial H}{\partial G(\theta)} = 0, \theta \in [0, h(0)] \tag{19a}$$
$$\frac{\partial H}{\partial G(\theta)} + \left[\frac{\partial H}{\partial \tilde{G}(t)}\frac{1}{1+\dot{h}(t)}\right]_{t=\theta-\sigma(\theta)} = 0, \theta \in [h(0), T] \tag{19b}$$
$$\left[\frac{\partial H}{\partial \tilde{G}(t)}\frac{1}{1+\dot{h}(t)}\right]_{t=\theta-\sigma(\theta)} = 0, \theta \in [T, T + h(T)] \tag{19c}$$

Applying similar reasoning to v and $\tilde{v}$[1], we have

$$\frac{\partial H}{\partial v(\theta)} = 0, \theta \in [0, h(0)] \tag{20a}$$

$$\frac{\partial H}{\partial v(\theta)} + \left[\frac{\partial H}{\partial \tilde{v}(t)} \frac{1}{1+\dot{h}(t)}\right]_{t=\theta-\sigma(\theta)} = 0, \ \theta \in [h(0), T] \tag{20b}$$

$$\left[\frac{\partial H}{\partial \tilde{v}(t)} \frac{1}{1+\dot{h}(t)}\right]_{t=\theta-\sigma(\theta)} = 0, \ \theta \in [T, T+h(T)] \tag{20c}$$

Note that $1+\dot{h}(t) > 0$ under FIFO, in line with (16), (19a), (19b), (20a), (20b), (19c) and (20c), we have the following stationary conditions:

$$\frac{\partial H}{\partial q(\theta)} = 0, \theta \in [0, T] \tag{21a}$$

$$\frac{\partial H}{\partial G(\theta)} + \left[\frac{\partial H}{\partial \tilde{G}(t)} \frac{1}{1+\dot{h}(t)}\right]_{t=\theta-\sigma(\theta)} = 0, \theta \in [h(0), T] \tag{21b}$$

$$\frac{\partial H}{\partial G(\theta)} = 0, \theta \in [0, h(0)] \tag{21c}$$

$$\frac{\partial H}{\partial v(\theta)} + \left[\frac{\partial H}{\partial \tilde{v}(t)} \frac{1}{1+\dot{h}(t)}\right]_{t=\theta-\sigma(\theta)} = 0, \theta \in [h(0), T] \tag{21d}$$

$$\frac{\partial H}{\partial v(\theta)} = 0, \theta \in [0, h(0)] \tag{21e}$$

$$\left[\frac{\partial H}{\partial \tilde{G}(t)}\right]_{t=\theta-\sigma(\theta)} = 0, \theta \in [T, T+h(T)] \tag{21f}$$

$$\left[\frac{\partial H}{\partial \tilde{v}(t)}\right]_{t=\theta-\sigma(\theta)} = 0, \theta \in [T, T+h(T)] \tag{21g}$$

Substituting (15b) and (15c) into (21b), we have

$$\alpha(\theta) = -\frac{\mu\left(\theta-\sigma(\theta)\right) v\left(\theta-\sigma(\theta)\right)}{1+\dot{h}\left(\theta-\sigma(\theta)\right)}, \theta \in [h(0), T] \tag{22}$$

Again, we would like to point out that we are tracing the history of the network to evaluate the effect of the amount of flow exiting the network at time θ. On the other hand, if the exit time (future) of vehicles entering the network at time θ is concerned, we can express (22) as

$$\alpha\left(\theta+h(\theta)\right) = -\frac{\mu(\theta)v(\theta)}{1+\dot{h}(\theta)}, \theta+h(\theta) \in [h(0), T] \tag{23}$$

Substituting (15e) and (15f) into (21d) yields

$$-\mu(\theta)\tilde{G}(\theta) + \xi(\theta) + \frac{\mu\left(\theta-\sigma(\theta)\right) q\left(\theta-\sigma(\theta)\right)}{1+\dot{h}\left(\theta-\sigma(\theta)\right)} = 0, \theta \in [h(0), T] \tag{24}$$

[1]For brevity, we have omitted the derivation.

Using (5) and noting that $\tilde{G}(\theta) = \frac{q(\theta)}{1+\dot{h}(\theta)}$, we can rewrite (24) as

$$\xi(\theta) = \frac{\mu(\theta)q(\theta)}{1+\dot{h}(\theta)} - \frac{\mu\left(\theta-\sigma(\theta)\right)q\left(\theta-\sigma(\theta)\right)}{1+\dot{h}\left(\theta-\sigma(\theta)\right)}, \theta \in [h(0), T] \tag{25}$$

According to (21c) and (15b)

$$\begin{aligned} \frac{\partial H}{\partial G(\theta)} &= -\alpha(\theta) = 0, \theta \in [0, h(0)] \\ \alpha(\theta) &= 0, \theta \in [0, h(0)] \end{aligned} \tag{26}$$

According to (21e) and (15e) we have

$$\begin{aligned} \frac{\partial H}{\partial v(\theta)} &= -\mu(\theta)\tilde{G}(\theta) + \xi(\theta) = 0, \theta \in [0, h(0)] \\ \xi(\theta) &= \mu(\theta)\tilde{G}(\theta) = \frac{\mu(\theta)q(\theta)}{1+\dot{h}(\theta)}, \theta \in [0, h(0)] \end{aligned} \tag{27}$$

From (21f) and (15c), we have

$$\left[\frac{\partial H}{\partial \tilde{G}(t)}\right]_{t=\theta-\sigma(\theta)} = -\mu(\theta-\sigma(\theta))v(\theta-\sigma(\theta)) = 0, \theta \in [T, T+h(T)]$$

regarding the entry time $\theta - \sigma(\theta)$. Or by time shifts

$$-\mu(\theta)v(\theta) = 0, \theta \in [T-\sigma(T), T] \tag{28}$$

regarding the current time θ. The physics of Condition (28) is that the network must be cleared at the end of the planning horizon, i.e., T, for the sake of flow conservation. Therefore, travelers are not allowed to depart later than $T - \sigma(T)$ to guarantee all travelers would arrive at their destination before T.

Similarly, from (21g) and (15f) one can get

$$\begin{aligned} \left[\frac{\partial H}{\partial \tilde{v}(t)}\right]_{t=\theta-\sigma(\theta)} &= \mu(\theta-\sigma(\theta))q(\theta-\sigma(\theta)) = 0, \theta \in [T, T+h(T)] \\ \mu(\theta)q(\theta) &= 0, \ \theta \in [T-\sigma(T), T] \end{aligned} \tag{29}$$

Combining (17a) and (15d) we obtain

$$\dot{\alpha}(\theta) = \xi(\theta)\frac{\partial \mathcal{V}(n(\theta))}{\partial n(\theta)}, \theta \in [0, T] \tag{30}$$

Integrating (23), (25), (26), (27) and (30), we have

$$\alpha(\theta) = \begin{cases} 0, & \theta \in [0, h(0)] \\ -\dfrac{\mu\left(\theta-\sigma(\theta)\right)v\left(\theta-\sigma(\theta)\right)}{1+\dot{h}\left(\theta-\sigma(\theta)\right)}, & \theta \in [h(0), T] \end{cases} \tag{31a}$$

$$\xi(\theta) = \begin{cases} \dfrac{\mu(\theta)q(\theta)}{1+\dot{h}(\theta)}, & \theta \in [0, h(0)] \\ \dfrac{\mu(\theta)q(\theta)}{1+\dot{h}(\theta)} - \dfrac{\mu\left(\theta-\sigma(\theta)\right)q\left(\theta-\sigma(\theta)\right)}{1+\dot{h}\left(\theta-\sigma(\theta)\right)}, & \theta \in [h(0), T] \end{cases} \tag{31b}$$

$$\dot{\alpha}(\theta) = \xi(\theta)\frac{\partial \mathcal{V}(n(\theta))}{\partial n(t)}, \theta \in [0, T] \tag{31c}$$

From (31a), (31b) and (29), if $\theta \in [T-\sigma(T), T]$, we have

$$\begin{aligned}\xi(\theta) &= \frac{\mu(\theta)q(\theta)}{1+\dot{h}(\theta)} - \frac{\mu\left(\theta-\sigma(\theta)\right)q\left(\theta-\sigma(\theta)\right)}{1+\dot{h}\left(\theta-\sigma(\theta)\right)} \\ &= 0 - \frac{\mu\left(\theta-\sigma(\theta)\right)q\left(\theta-\sigma(\theta)\right)}{1+\dot{h}\left(\theta-\sigma(\theta)\right)} \\ &= \frac{q\left(\theta-\sigma(\theta)\right)}{v\left(\theta-\sigma(\theta)\right)}\alpha(\theta), \theta \in [T-\sigma(T), T] \end{aligned} \tag{32}$$

Substituting (31c) into (32) results in

$$\begin{aligned}\dot{\alpha}(\theta) &= \frac{q\left(\theta-\sigma(\theta)\right)}{v\left(\theta-\sigma(\theta)\right)}\alpha(\theta)\frac{\partial \mathcal{V}(n(\theta))}{\partial n(\theta)}, \theta \in [T-\sigma(T), T] \\ \alpha(\theta) &= \tilde{c}\exp\left(\int \frac{q\left(\theta-\sigma(\theta)\right)}{v\left(\theta-\sigma(\theta)\right)}\frac{\partial \mathcal{V}(n(\theta))}{\partial n(\theta)}\mathrm{d}\theta\right)\end{aligned}$$

From (31a) and (28), we have $\alpha(T) = 0$. This together with

$$\exp\left(\int \frac{q\left(\theta-\sigma(\theta)\right)}{v\left(\theta-\sigma(\theta)\right)}\frac{\partial \mathcal{V}(n(\theta))}{\partial n(\theta)}\mathrm{d}\theta\right) \neq 0,$$

implies $\tilde{c} = 0$. Therefore,

$$\alpha(\theta) = 0, \theta \in [T-\sigma(T), T] \tag{33}$$

From (31a) and (31b), if $\theta \in [h(0), T-\sigma(T)]$, we have

$$\begin{aligned}\xi(\theta) &= \frac{\mu(\theta)q(\theta)}{1+\dot{h}(\theta)} - \frac{\mu\left(\theta-\sigma(\theta)\right)q\left(\theta-\sigma(\theta)\right)}{1+\dot{h}\left(\theta-\sigma(\theta)\right)} \\ &= \frac{q(\theta)}{v(\theta)}\frac{\mu(\theta)v(\theta)}{1+\dot{h}(\theta)} - \frac{\mu\left(\theta-\sigma(\theta)\right)q\left(\theta-\sigma(\theta)\right)}{1+\dot{h}\left(\theta-\sigma(\theta)\right)} \\ &= -\frac{q(\theta)}{v(\theta)}\alpha\left(\theta+h(\theta)\right) + \frac{q\left(\theta-\sigma(\theta)\right)}{v\left(\theta-\sigma(\theta)\right)}\alpha(\theta), \quad \theta \in [h(0), T-\sigma(T)]\end{aligned} \tag{34}$$

From (34), we notice that $\xi(\theta)$, the Lagrange multiplier associated with the speed-MFD for vehicles entering the network at time θ, depends on both the network memory from $\theta-\sigma(\theta)$ to θ and future network state from θ to $\theta+h(\theta)$. This is because the network accumulation $n(\theta)$ is determined by the network memory from $\theta-\sigma(\theta)$ to θ according to the flow conservation. During the vehicles' presence in the network, their trip duration $h(\theta)$ is a result of the "future" network speed till they exit from the network by (2).

Substituting (31c) into (34) results in

$$\dot{\alpha}(\theta) = \left[-\frac{q(\theta)}{v(\theta)}\alpha\left(\theta+h(\theta)\right) + \frac{q\left(\theta-\sigma(\theta)\right)}{v\left(\theta-\sigma(\theta)\right)}\alpha(\theta)\right]\frac{\partial \mathcal{V}(n(\theta))}{\partial n(\theta)}, \theta \in [h(0), T-\sigma(T)] \tag{35}$$

Now suppose the following conditions hold for an instant $tt \leq T-\sigma(T)$ satisfying $tt+h(tt) \in [tt, T]$ and

$$\alpha(\theta) = 0, \theta \in [tt, T]$$

There is an infinitesimal Δtt such that

$$tt - \Delta tt + h(tt - \Delta tt) \in [tt, T]$$

Obviously, any $\Delta tt \leq \sigma(tt)$ can fulfil the above requirement.

Now consider $\theta \in [tt - \Delta tt, tt]$, note $\theta + h(\theta) \in [tt - \Delta tt + h(tt - \Delta tt), tt + h(tt)] \subset [tt, T]$, we have $\alpha(\theta + h(\theta)) = 0$. From (35) we have:

$$\dot{\alpha}(\theta) = -\frac{q(\theta)}{v(\theta)}\frac{\partial \mathcal{V}(n(\theta))}{\partial n(\theta)}\alpha\left(\theta + h(\theta)\right) + \frac{q\left(\theta - \sigma(\theta)\right)}{v\left(\theta - \sigma(\theta)\right)}\frac{\partial \mathcal{V}(n(\theta))}{\partial n(\theta)}\alpha(\theta) = \frac{q\left(\theta - \sigma(\theta)\right)}{v\left(\theta - \sigma(\theta)\right)}\frac{\partial \mathcal{V}(n(\theta))}{\partial n(\theta)}\alpha(\theta)$$

$$\alpha(\theta) = \tilde{c}\exp\left(\int \frac{q\left(\theta - \sigma(\theta)\right)}{v\left(\theta - \sigma(\theta)\right)}\frac{\partial \mathcal{V}(n(\theta))}{\partial n(\theta)}\mathrm{d}\theta\right)$$

Note $\alpha(tt) = 0$. This together with $\exp\left(\int \frac{q(\theta-\sigma(\theta))}{v(\theta-\sigma(\theta))}\frac{\partial \mathcal{V}(n(\theta))}{\partial n(\theta)}\mathrm{d}\theta\right) \neq 0$, implies $\tilde{c} = 0$. Therefore,

$$\alpha(\theta) = 0, \theta \in [tt - \Delta tt, tt] \tag{36}$$

To sum up, we have

$$\alpha(\theta) = 0, \theta \in [tt - \Delta tt, T]$$

for $t \in [tt - \Delta tt, T]$. It has been proven earlier that $\alpha(t) = 0$, and noting that $[T - \sigma(T), T] \subseteq [tt - \Delta tt, T]$ with tt arbitrarily chosen. We can expand this time interval to the entire planning horizon $[0, T]$. This gives

$$\alpha(t) = 0, t \in [h(0), T]$$

With (31a), we have

$$\alpha(t) = 0, t \in [0, T]$$

Further, we have

$$\mu(t) = 0, t \in [0, T] \tag{37}$$

From (15a) and (16), we have the following condition at the equilibrium

$$\Psi(v^*, t) + \alpha(t) + \rho(t) + \mu(t)\tilde{v}(t) - \gamma(t) + \zeta(t) = 0, t \in [0, T]$$

Using (15g), (17b) and the boundary condition (18), we have

$$\rho(t) = \rho(T) = -\phi$$

Therefore,

$$\Psi(v^*, t) - \gamma(t) + \zeta(t) = \phi, \ t \in [0, T]$$

Note that $\gamma(t)$ is the Lagrange multiplier associated with the nonnegative flow constraint. Whenever there is a departure, we have $q(t) > 0$ and thus $\gamma(t) = 0$. We now can summarize the equilibrium condition for the basic trip-based model with departure time choice as

$$q(t)\begin{cases} > 0, \Psi(v^*, t) + \zeta(t) = \phi \\ = 0, \Psi(v^*, t) + \zeta(t) > \phi \end{cases} \tag{38}$$

where ϕ is the equilibrium travel cost, $\zeta(t)$ is the additional cost caused by the traffic control via imposing an upper bound constraint on the inflow rate. When there is no upper bound constraint on the inflow rate, we have

$$q(t)\begin{cases} > 0, \Psi(v^*, t) = \phi \\ = 0, \Psi(v^*, t) > \phi \end{cases} \tag{39}$$

■

Remark 3.2. As we can see from the above proof and the discussion in Section 2, due to the difference in evaluating travel time for these two classes of MFD models, the information support should be also different. In the accumulation-based model, the travel time and thus the travel cost is determined by the current traffic state. Travelers choose their departure times according to the travel cost perceived. On the other hand, the travel cost of trip-based model depends on the "future state" information (i.e., the traffic state throughout the trip duration). We need to predict the traffic state (speed to be exact) during the trip to infer the travel time to support the departure time choice for travelers. However, accurate prediction of future traffic state is never easy unless it is a pure connected automated vehicle environment (Zhong et al., 2017). Or, we can apply the trip-based model for off-line applications that the optimization is based on the historical traffic pattern. ∎

4. Numerical examples

Numerical examples are conducted to demonstrate the properties of DUE with the basic trip-based model with respect to different test scenarios in this section. The solution algorithm is outlined in the appendix. Consider an urban network admitting a well-defined MFD widely used in the literature (Geroliminis et al., 2013), e.g., $G(n) = (1.4877\times10^{-7}\times n^3 - 2.9815\times10^{-3}\times n^2 + 15.0912\times n)/3600$, with $G^{max} = 6.3$ (unit/time). The traffic state within the basic trip-based model is given by a well-defined relationship between the travel production $P(n(t))$ and the accumulation $n(t)$. Note that the travel production $P(n(t))$ is the distance of all vehicles in a unit time, we have the relationship between the mean speed $\mathcal{V}(n(t))$ and the travel production $P(n(t))$ as $P(n(t)) = \mathcal{V}(n(t))\, n(t)$. According to Daganzo (2007); Mariotte et al. (2017), the trip length L is the same for all travelers and satisfies $G(n(t)) = P(n(t))/L$. Then we have the following equation:

$$\mathcal{V}(n(t))\, n(t) = P(n(t)) = G(n(t))\, L \tag{40}$$

to extract the speed-MFD from the accumulation MFD. Following this, we have $\mathcal{V}(n) = 1.4877\times10^{-7}\times n^2 - 2.9815\times10^{-3}\times n + 15.0912$ (unit-legnth/unit-time), with free flow velocity $\mathcal{V}(0) = 15.0912$ (unit-legnth/unit-time). The trip length is $L = 3600$ (unit-length), while the region free flow travel time is $L/\mathcal{V}(0)$, around 238 unit-times. Total amount of within-region demand to be assigned is $Q = 1500$ (units). The planning horizon is set at $T = 800$ (unit-times) to ensure all travel demand can be served. The upper bound of inflow rate is set as 6.3 (unit/time), i.e., the capacity. Early/late arrival penalty is defined as

$$\kappa[\chi] = \begin{cases} 0.1(t + h(t) - t_{de})^2, & t + h(t) < t_{de} \\ 0, & t_{de} \le t + h(t) \le t_{dl} \\ 0.1(t + h(t) - t_{dl})^2, & t + h(t) > t_{dl} \end{cases} \tag{41}$$

with expected arrival time window ranging from $[t_{de}, t_{dl}] = [400, 600]$ (unit-time).

Solving the DUE with departure time choice only, we depict the inflow rate against the corresponding travel cost over time and the number of vehicles in Figure 2(a)-Figure 2(b), respectively. The generalized travel cost (including the travel time, schedule penalty, and the additional cost induced by the inflow upper bound) and the path flow during the departure window fulfill the DUE condition as outlined in (13). The departure time window is larger than the preferred departure window (with zero schedule penalty). This is because travelers choose their departure times to minimize the generalized travel cost and also try to avoid the additional cost induced by the saturated inflow constraint. Note that there is no route choice but departure time choice for within-region case, it is similar to the perimeter control located at a regional border, that manipulates the transfer flows across the border to optimize the regional operational performance, with

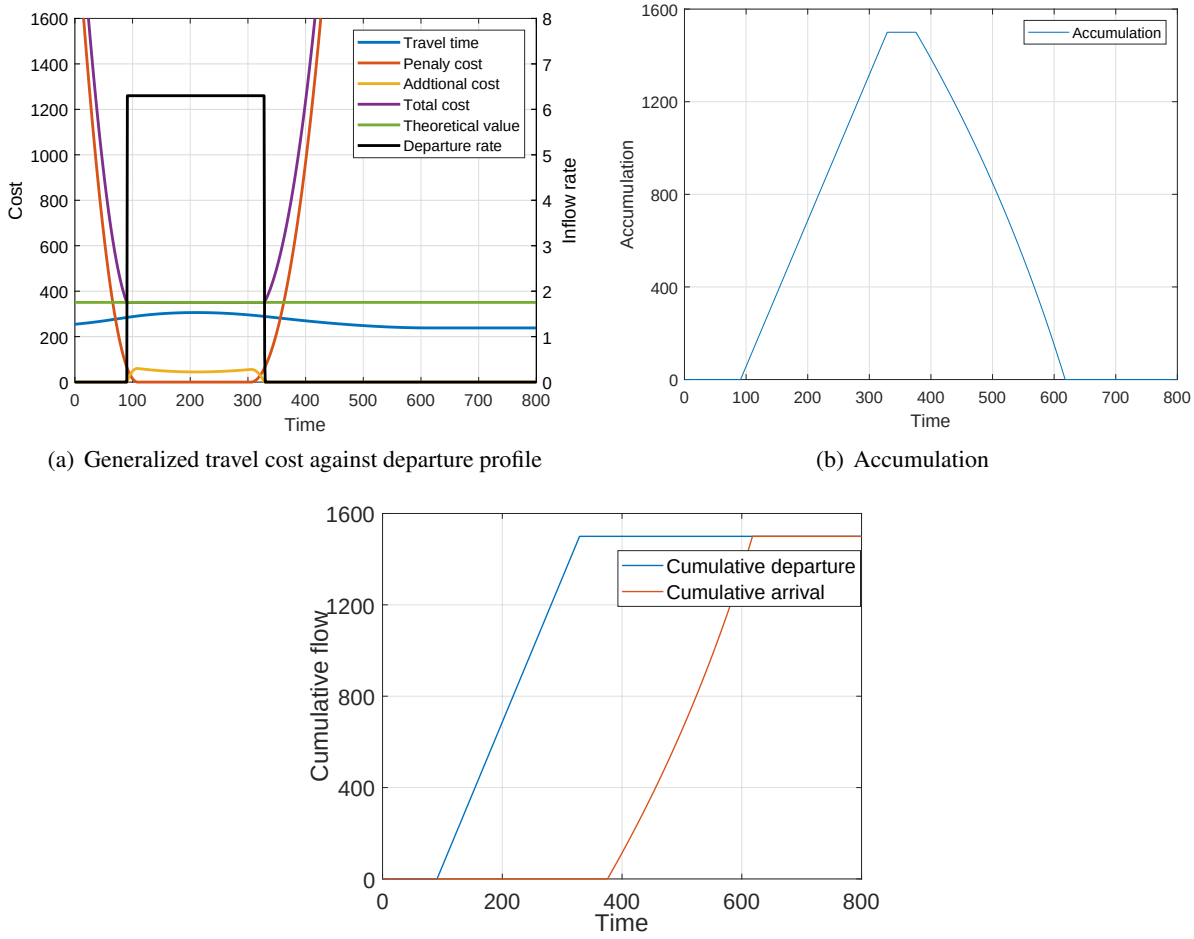

(a) Generalized travel cost against departure profile

(b) Accumulation

(c) Cumulative departures and arrivals

Figure 2: Generalized travel cost against departure profile and number of vehicles with constraint

control input saturation as investigated in Haddad (2017a,b). The inflow profile depicted in Figure 2(a) is similar to the Bang-bang like optimal control law obtained in the conventional optimal control formulations of gating control (Haddad, 2017a; Zhong et al., 2018a). Similar observation is also achieved for the DUE problem with departure time choice using the accumulation-based MFD system with time delay as the network loading model (Huang et al., 2020). Despite their similarity, we would like to point out that there is no guarantee that the optimal departure rate will be the Bang-bang law as achieved in the conventional optimal control formulations of gating control. Interested readers can refer to Huang et al. (2020) for details.

The difference between the trip-based model and the accumulation-based MFD model in terms of flow propagation and travel time evaluation can also result in a very different treatment on the inflow capacity constraint. In the accumulation-based MFD dynamics, the travel time is determined by the network state at the instant when the vehicle enters the network, i.e., (1). We need an upper bound (explicitly or implicitly) to restrict the departure rate to avoid the situation that all vehicles rush into the network at the moment when the minimum travel cost is first achieved (Zhong et al., 2011; Han et al., 2019; Huang et al., 2020). On the other hand, the travel time of trip-based model is a result of the network traffic speed throughout the trip duration, i.e., (2). The trip-based MFD model do not need such an upper bound to ensure a proper DUE

pattern since too large inflow rate would result in a very large travel time rendering the cost and flow could not form a UE pattern. To see this, we remove the upper bound inflow constraint to test the unconstrained UE pattern. Figure 3(a) depicts the departure flow profile against the travel cost profile while Figure 3(b) presents the evolution trajectory of corresponding number of vehicles. As we can see, once the minimum cost is achieved, a departure rate around 24.6 (units/unit-time) rush into the network (around three times the network inflow capacity). The travel cost increases with respect to the accumulation in the network. The inflow rate must then decline to maintain a low cost level. After a while, an amount of vehicles complete their trips. The travel cost profile would decrease again. As a consequence, the departure rate would admit an increase till all the demand is served. This results in two peaks in the departure profile and two flats in the number of vehicles. It is also possible that two peaks in the vehicle accumulation can be observed if the departure time window is large enough. On the other hand, the UE cost pattern is not as ideal as that of the constrained one. This highlights the benefit of introducing inflow capacity constraint, i.e., not only making the problem more physically meaningful but also preventing the undesired phenomenon of two peaks in the departure profile and vehicle accumulation.

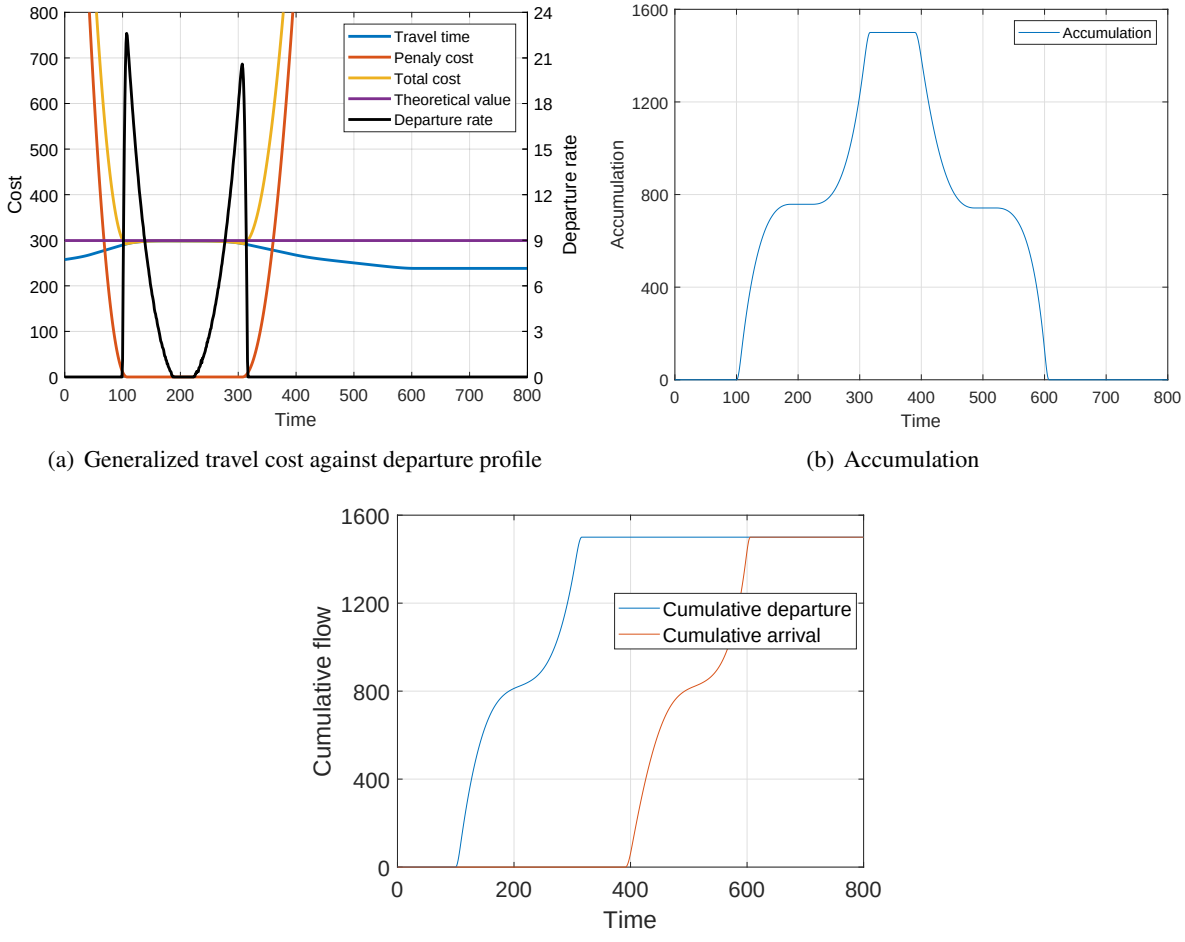

(a) Generalized travel cost against departure profile

(b) Accumulation

(c) Cumulative departures and arrivals

Figure 3: Generalized travel cost against departure profile and number of vehicles without constraint

Regarding the above discussion in Remark 3.2, the departure rate constraint imposed in this example

can somehow alleviate the information support required by the trip-based model. When the departure rate constraint is activated, the inflow rate to the network is certain (i.e., the upper bound). Thus the network traffic state, travel time, and schedule penalty are easy to obtain. The additional cost induced by the departure rate constraint is determined by the Lagrange multiplier. Thus the DUE cost under this case can be obtained quite easily. On the other hand, for the unconstrained case, the travel cost of trip-based model depends on not only the current traffic state (as a result of the historical inflow profile) but also the "future" traffic state throughout the trip duration as discussed in Section 2. Assessing the travel cost in this manner is very difficult. Therefore, it is more difficult to obtain a good dynamic user equilibrium as shown in Figure 3(a).

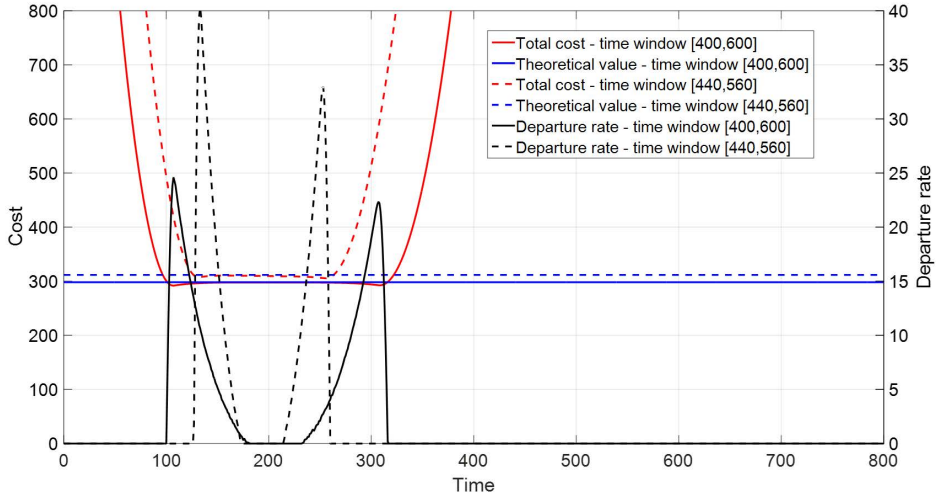

Figure 4: The effect of desired arrival time window on generalized travel cost and departure profile: unconstrained case

To test the effect of desired arrival time window on the generalized travel cost and the departure profile, we assume the desired arrival time window is $[440, 560]$ (unit-time) and adopt the same settings for other parameters. For the unconstrained case, as we can see from Figure 4, compared with the previous case with the desired arrival time window as $[400, 600]$, smaller the time window is, higher the departure flow rate is. This is because the travel demand is squeezed into a narrower departure time window to achieve the DUE. Thus larger travel time is incurred and higher DUE cost would be yielded.

To test the effect of desired arrival time window and the upper bound constraint on the generalized travel cost and the departure profile, we test the combinations of the desired arrival time windows $[440, 560]$ and $[400, 600]$ (unit-time) with the upper bound constraints 6.3 and 7.56 (20% above the capacity). We would like to point out that although the physical meaning of the upper bound constraint is regarded as the network capacity, we only change the upper bound constraint in the tests while keeping the MFD unchanged for a fair comparison. Figure 5 shows that, under the same desired arrival time window, the additional cost caused by the upper bound constraint increases sharply as the upper bound constraint decreases. On the other hand, assuming the upper bound constraint is 9.45 (50% above the capacity), Figure 6 indicates that, with the same upper bound constraint, the width of the desired arrival time window has a strong impact on the additional cost. The additional cost increases as the desired arrival time window becomes smaller.

Given the travel demand, the congestion level depends on the inflow capacity constraint and the desired arrival time window (within which no schedule penalty would be occurred). For the first test scenario wherein the inflow capacity constraint is 6.3 and the desired arrival time window is 200, the travel demand 1500 is (16 %) larger than the nominal network capacity 1260 (i.e., 6.3×200). Therefore, the additional

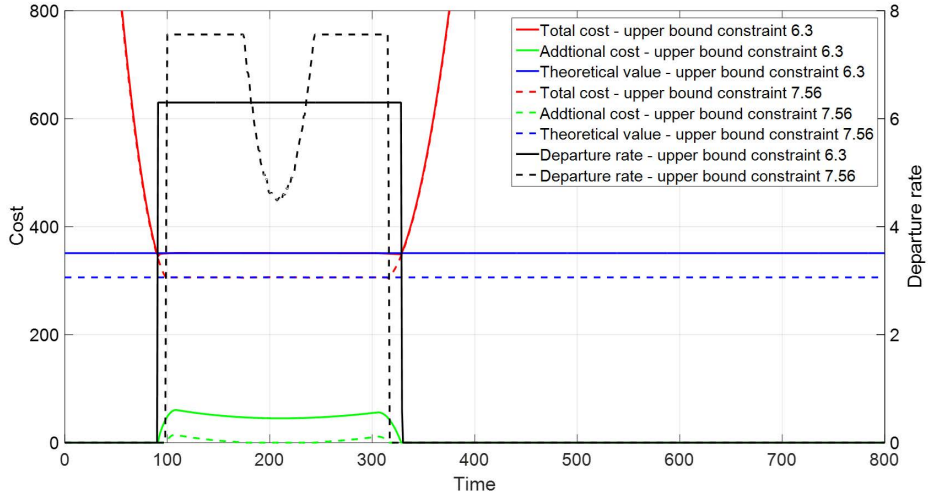

Figure 5: The effect of upper bound constraint on generalized travel cost and additional cost with arrival time window $[400, 600]$

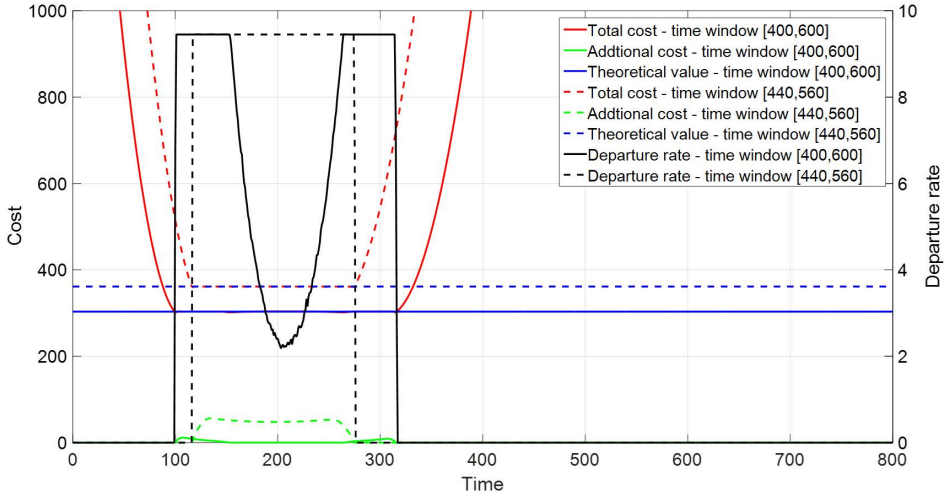

Figure 6: The effect of desired arrival time window on generalized travel cost and additional cost

cost caused by the inflow capacity constraint is quite large and its average scope is around 13.6 % of the DUE cost, see Figure 2(a). For the case when the inflow capacity constraint is 7.56 and the desired arrival time window is 200, the travel demand 1500 is slightly less than the nominal network capacity 1512 (i.e., 7.56×200). Therefore, we can observe two peaks in the departure flow profile while the additional cost caused by the inflow capacity constraint is small, see Figure 5. For the case when the inflow capacity constraint is 9.45 and the desired arrival time window is 120, the travel demand 1500 is (24.4 %) larger than the nominal network capacity 1134. The additional cost of this case is around 13% of the DUE cost. This example suggests that, given large enough desired arrival time window (i.e., ensuring the feasibility of the DUE problem), the inflow capacity constraint may have a stronger effect on the additional cost than the desired arrival time window. However, we cannot conclude this as a general rule from such limited samples

on the one hand. On the other hand, the physical meaning of the inflow capacity constraint is the maximum throughput of the accumulation MFD (which is converted into speed MFD by (40)). When we increase the inflow capacity constraint to 9.45, we do not change the accumulation MFD accordingly so as to perform a fair comparison in the sensitivity analysis.

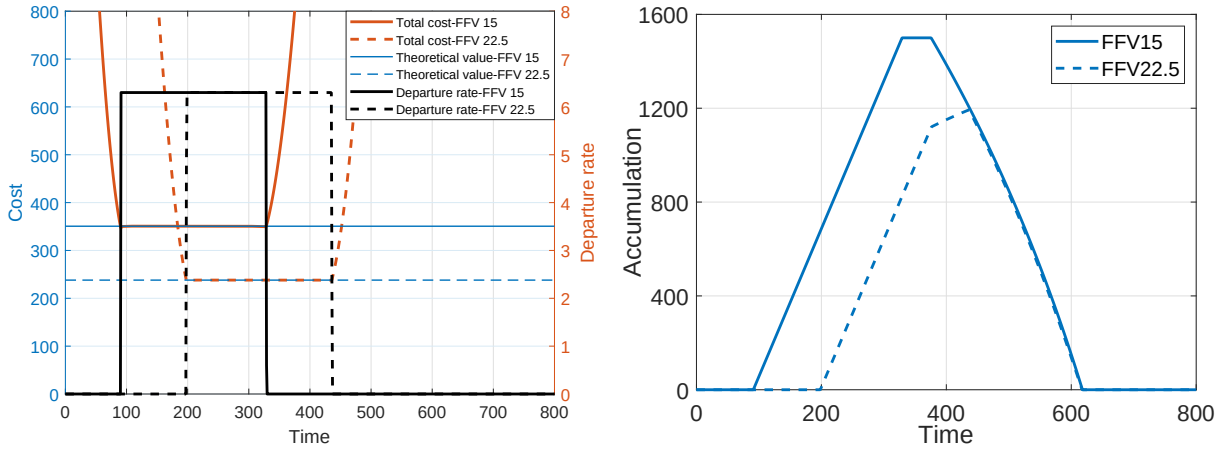

(a) Generalized travel cost against departure profile

(b) Accumulation

Figure 7: The effect of MFD parameters on generalized travel cost and additional cost

Modify the MFD by times 1.5

To test the effect of MFD parameters on the generalized travel cost and the departure profile, we assume a network with the free flow speed 1.5 times faster than in Figure 2 while the upper bound and other settings stay unchanged for a fair comparison. As shown in Figure 7(a), the DUE conditions are well-satisfied in both scenarios while the departure time in the network with higher speed postponed later than the original network. An interpretation of this phenomenon is that travelers in the network with better infrastructure have the freedom to depart late and access to smoother traffic state as shown in Figure 7(b). This supports the investment in infrastructure construction and development.

5. Conclusions

Recently, the trip-based MFD models, which are claimed to be more accurate than the conventional accumulation-based MFD model especially during transient phases, is used to replace the Vickrey's bottleneck model to simulate the hyper-congestion in rush-hour traffic dynamics by both transportation scientists and urban transportation economists. But every coin has two sides: while the trip-based model can better capture the hyper-congestion it also introduces significant mathematical difficulties that preclude straightforward analytical and numerical solutions (Arnott and Buli, 2018). This paper investigated the dynamic user equilibrium of departure time choice in an isotropic urban network with identical travelers using the basic trip-based model. Parallel to the numerical treatments developed in the literature, analytical DUE conditions under general travel time function and schedule penalty function were derived. Under dynamic user equilibrium, no traveler can reduce her/his travel cost by changing the departure time. The derivation does not rely on some common assumptions in the literature such as linear travel cost function, no late arrivals, and linear speed-MFD. Numerical examples verified theoretical developments. It is demonstrated that the width of the desired arrival time window can lead to a unimodal evolution of accumulation but two

peaks in the departure profile depending on the demand level under the same network configuration, e.g., the inflow capacity constraint. The numerical results also demonstrate that the inflow capacity constraint can prevent the two peaks in the departure profile and vehicle accumulation meanwhile generating a better DUE pattern. Extending the analysis for trip-based models with heterogeneous trip lengths, solving for the social optimum and pricing applications would be interesting future works.

Acknowledgments

Financial support from the National Natural Science Foundation of China (No. 72071214), the National Key R&D Program of China (No. 2018YFB1600500), the Research Grants Council of Hong Kong (No. 15211518E), and the CCF-DiDi Big-Data Joint Lab is gratefully acknowledged.

References

Aghamohammadi, R. and Laval, J. A., 2020. Dynamic traffic assignment using the macroscopic fundamental diagram: A review of vehicular and pedestrian flow models. *Transportation Research Part B: Methodological*, 137:99 – 118.

Amirgholy, M. and Gao, H. O., 2017. Modeling the dynamics of congestion in large urban networks using the macroscopic fundamental diagram: User equilibrium, system optimum, and pricing strategies. *Transport. Res. Part B*, 104:215–237.

Arnott, R., 2013. A bathtub model of downtown traffic congestion. *J Urban Econ*, 76(4):110–121.

Arnott, R. and Buli, J., 2018. Solving for equilibrium in the basic bathtub model. *Transport. Res. Part B*, 109:150–175.

Arnott, R., Kokoza, A., and Naji, M., 2016. Equilibrium traffic dynamics in a bathtub model: A special case. *Economics of transportation*, 7:38–52.

Buisson, C. and Ladier, C., 2009. Exploring the Impact of Homogeneity of Traffic Measurements on the Existence of Macroscopic Fundamental Diagrams. *Transport. Res. Rec.*, (2124):127–136.

Daganzo, C. F., 2007. Urban gridlock: Macroscopic modeling and mitigation approaches. *Transport. Res. Part B*, 41(1):49–62.

Daganzo, C. F. and Geroliminis, N., 2008. An analytical approximation for the macroscopic fundamental diagram of urban traffic. *Transport. Res. Part B*, 42(9):771–781.

Daganzo, C. F. and Lehe, L. J., 2015. Distance-dependent congestion pricing for downtown zones. *Transport. Res. Part B*, 75: 89–99.

Fosgerau, M., 2015. Congestion in the bathtub. *Economics of Transportation*, 4(4):241–255.

Fosgerau, M. and Small, K. A., 2013. Hypercongestion in downtown metropolis. *Journal of Urban Economics*, 76:122 – 134.

Friesz, T. L. and Han, K., 2019. The mathematical foundations of dynamic user equilibrium. *Transportation research part B: methodological*, 126:309–328.

Geroliminis, N. and Daganzo, C. F., 2008. Existence of urban-scale macroscopic fundamental diagrams: Some experimental findings. *Transport. Res. Part B*, 42(9):759–770.

Geroliminis, N. and Sun, J., 2011. Hysteresis phenomena of a macroscopic fundamental diagram in freeway networks. *Transport. Res. Part A*, 45(9):966–979.

Geroliminis, N., Haddad, J., and Ramezani, M., 2013. Optimal perimeter control for two urban regions with macroscopic fundamental diagrams: A model predictive approach. *IEEE Trans. Intell. Transp. Syst.*, 14(1):348–359.

Haddad, J., 2017a. Optimal coupled and decoupled perimeter control in one-region cities. *Control Eng. Pract.*, 61:134–148.

Haddad, J., 2017b. Optimal perimeter control synthesis for two urban regions with aggregate boundary queue dynamics. *Transport. Res. Part B*, 96:1–25.

Haddad, J. and Mirkin, B., 2016. Adaptive perimeter traffic control of urban road networks based on MFD model with time delays. *Int J Robust Nonlin*, 26(6):1267–1285.

Haddad, J. and Zheng, Z., 2020. Adaptive perimeter control for multi-region accumulation-based models with state delays. *Transportation Research Part B: Methodological*, 137:133 – 153.

Han, K., Eve, G., and Friesz, T. L., 2019. Computing dynamic user equilibria on large-scale networks with software implementation. *Networks and Spatial Economics*, 19(3):869–902.

Huang, Y., Xiong, J., Sumalee, A., Zheng, N., Lam, W., He, Z., and Zhong, R., 2020. A dynamic user equilibrium model for multi-region macroscopic fundamental diagram systems with time-varying delays. *Transportation Research Part B: Methodological*, 131:1–25.

Keyvan-Ekbatani, M., Kouvelas, A., Papamichail, I., and Papageorgiou, M., 2012. Exploiting the fundamental diagram of urban networks for feedback-based gating. *Transport. Res. Part B*, 46(10):1393–1403.

Lamotte, R. and Geroliminis, N., 2018. The morning commute in urban areas with heterogeneous trip lengths. *Transport. Res. Part B*, 117:794–810.

Li, C. and Huang, H., 2019. Analysis of bathtub congestion with continuous scheduling preference. *Research in Transportation Economics*, 75:45–54.

Li, C.-Y. and Huang, H.-J., 2017. Morning commute in a single-entry traffic corridor with early and late arrivals. *Transportation Research Part B: Methodological*, 97:23–49.

Li, C.-Y. and Huang, H.-J., 2018. User equilibrium of a single-entry traffic corridor with continuous scheduling preference. *Transportation Research Part B: Methodological*, 108:21–38.

Mariotte, G. and Leclercq, L., 2019. Flow exchanges in multi-reservoir systems with spillbacks. *Transport. Res. Part B*, 122: 327–349.

Mariotte, G., Leclercq, L., and Laval, J. A., 2017. Macroscopic urban dynamics: Analytical and numerical comparisons of existing models. *Transport. Res. Part B*, 101:245–267.

Mirkin, B., Haddad, J., and Shtessel, Y., 2016. Tracking with asymptotic sliding mode and adaptive input delay effect compensation of nonlinearly perturbed delayed systems applied to traffic feedback control. *Int J Control*, (9):1–20.

Ni, W. and Cassidy, M., 2020. City-wide traffic control: Modeling impacts of cordon queues. *Transportation Research Part C: Emerging Technologies*, 113:164 – 175.

Paipuri, M. and Leclercq, L., 2020. Bi-modal macroscopic traffic dynamics in a single region. *Transportation research part B: methodological*, 133:257–290.

Saberi, M., Mahmassani, H. S., Hou, T., and Zockaie, A., 2014. Estimating network fundamental diagram using three-dimensional vehicle trajectories: extending Edie's definitions of traffic flow variables to networks. *Transport. Res. Rec.*, (2422):12–20.

Small, K. A. and Chu, X., 2003. Hypercongestion. *Journal of Transport Economics and Policy*, 37(3):319–352.

Vickrey, W. S., 1969. Congestion Theory and Transport Investment. *Am Econ Rev*, 59(2):251–260.

Yildirimoglu, M. and Geroliminis, N., 2014. Approximating dynamic equilibrium conditions with macroscopic fundamental diagrams. *Transport. Res. Part B*, 70:186–200.

Yildirimoglu, M., Ramezani, M., and Geroliminis, N., 2015. Equilibrium analysis and route guidance in large-scale networks with MFD dynamics. *Transport. Res. Part C*, 59:404–420.

Yildirimoglu, M., Sirmatel, I. I., and Geroliminis, N., 2018. Hierarchical control of heterogeneous large-scale urban road networks via path assignment and regional route guidance. *Transport. Res. Part B*, 118:106–123.

Zhong, R., Sumalee, A., Friesz, T. L., and Lam, W. H. K., 2011. Dynamic user equilibrium with side constraints for a traffic network: Theoretical development and numerical solution algorithm. *Transport. Res. Part B*, 45(7):1035–1061.

Zhong, R., Luo, J., Cai, H., Sumalee, A., Yuan, F., and Chow, A. H. F., 2017. Forecasting journey time distribution with consideration to abnormal traffic conditions. *Transport. Res. Part C*, 85:292–311.

Zhong, R., Chen, C., Huang, Y., Sumalee, A., Lam, W., and Xu, D., 2018a. Robust perimeter control for two urban regions with macroscopic fundamental diagrams: A control-lyapunov function approach. *Transport. Res. Part B*, 117:687–707.

Zhong, R., Huang, Y., Chen, C., Lam, W., Xu, D., and Sumalee, A., 2018b. Boundary conditions and behavior of the macroscopic fundamental diagram based network traffic dynamics: A control systems perspective. *Transport. Res. Part B*, 111:327–355.

Appendix A. Solution algorithm

For demonstration purpose, we adopt the time-discretization based solution algorithm for the DUE problem using the MFD systems with time-varying delays as the network loading model developed in Huang et al. (2020). The essential difference lies in the network loading models, i.e., trip-based model in this paper and the accumulation-based model with time delays in Huang et al. (2020). As discussed in Zhong et al. (2011); Huang et al. (2020), the DUE problem cannot be solved by the optimal control formulation directly but through an iterative optimal control problem (or a fixed point algorithm) as depicted in Algorithm 1. To begin with, we summarize the nomenclature used in the algorithms in Table A.2.

Table A.2: Nomenclature used in Algorithms 1 – 3

l	Current iteration index
$I_{\max}$	Maximum iteration number
q^*	Optimal inflow profiles of DUE problem
q^l	Optimal inflow profiles of l^{th} subproblem
Ψ^l	Cost of q^l
ε	Tolerance of iteration
ϖ	Scalar parameter of the fixed-point problem
Δt	Time discretization
Δn	Vehicle discretiaztion
N	The number of discrete-time intervals
k_t	Index of discrete-time interval
$\tau_{\text{in}}(k_t)$	Entry time of time interval k_t
q_{k_t}	Departure rate of time interval k_t
$\tau_{\text{out}}(k_t)$	Exit time of vehicles entering at time $\tau_{\text{in}}(k_t)$
h_{k_t}	Travel time of vehicles entering at time $\tau_{\text{in}}(k_t)$
$Q_{\text{in}}(k_t)$	Cumulative inflow up to time $\tau_{\text{in}}(k_t)$
$Q_{\text{out}}(k_t)$	Cumulative outflow up to time $\tau_{\text{in}}(k_t)$
$\mathcal{V}(n)$	Speed-MFD
t_{in}	Current entry time
t_{out}	Current exit time
n_{in}	Accumulation at time t_{in}
n_{out}	Accumulation at time t_{out}
v_{in}	Speed at time t_{in}
v_{out}	Speed at time t_{out}
a	Arrive rate at time t_{out}
$Q^{\text{in}}_{t_{\text{in}}}$	Cumulative inflow up to time t_{in}
$Q^{\text{out}}_{t_{\text{in}}}$	Cumulative outflow up to time t_{in}
$Q^{\text{in}}_{t_{\text{out}}}$	Cumulative inflow up to time t_{out}
$Q^{\text{out}}_{t_{\text{out}}}$	Cumulative outflow up to time t_{out}

Algorithm 1 Fixed point algorithm for the DUE problem

Input: Maximum iteration number $I_{\max}$, tolerance $\varepsilon \in R_+$, parameter $\varpi \in R_+$

Output: optimal inflow profiles q^*

1: Initialization: iteration index $l = 0$, initial feasible solution q^0

2: **repeat**

3: $l = l + 1$

4: Optimal control subproblem. Solve

$$q^l = \arg\min_q \frac{1}{2} \int_0^T \left[q^{l-1} - \varpi \Psi^{l-1} - q \right]^2 \mathrm{d}t$$

where Ψ^l as evaluated by Algorithm 2 is the travel cost associated with the inflow profiles q^l, and q lies in the following set

$$\left\{ q : -q(t) \le 0, \quad q(t) \le q_{max}, \int_0^T q(t)\,\mathrm{d}t = Q, \ \forall t \in [0, T] \right\}.$$

5: **until** $l > I_{\max}$ or $\frac{\|q^{l+1} - q^l\|}{\|q^l\|} \le \varepsilon$

6: **return** optimal inflow profile $q^* = q^l$

Algorithm 2 Region loading

Input: time discretization Δt, vehicle discretization Δn, departure rate $q(t)$

Output: Travel time h_{k_t} $(k_t = 1, 2, \cdots, N)$

Initialization: number of time intervals $N = T/\Delta t$, entry time $\tau_{\text{in}}(k_t)$ $(k_t = 1, 2, \cdots, N, N+1)$ and departure rate q_{k_t} $(k_t = 1, 2, \cdots, N)$

$$\tau_{\text{in}}(k_t) = (k_t - 1)\Delta t, \quad q_{k_t} = q\left(\tau_{\text{in}}(k_t)\right)$$

Cumulative inflow $Q_{\text{in}}(k_t)$ $(k_t = 1, 2, \cdots, N, N+1)$

$$Q_{\text{in}}(k_t) = \sum_{k=1}^{k_t - 1} q_{k_t} \Delta t$$

Cumulative outflow $Q_{\text{out}}(1) = 0$

Initialization: current entry time $t_{\text{in}} = \tau_{\text{in}}(1)$, current exit time $t_{\text{out}} = \tau_{\text{in}}(1) + h_1$

for $k_t = 1$ to N **do**

  if $q_{k_t} = 0$ **then**

    Calculate n_{in} (accumulative at time t_{in}), and n_{out} (accumulative at time t_{out}) by Algorithm 3

    Calculate v_{in}(speed at time t_{in}) and v_{out} (speed at time t_{out})

$$v_{\text{in}} = \mathcal{V}(n_{\text{in}}), \quad v_{\text{out}} = \mathcal{V}(n_{\text{out}})$$

    Update t_{in} and t_{out}: $t_{\text{in}} = t_{\text{in}} + \Delta t$, $t_{\text{out}} = t_{\text{out}} + \frac{v_{\text{in}}}{v_{\text{out}}} \Delta t$

  else

    repeat

      Calculate n_{in} (accumulative at time t_{in}), and n_{out} (accumulative at time t_{out}) by Algorithm 3

      Calculate v_{in}(speed at time t_{in}) and v_{out} (speed at time t_{out})

$$v_{\text{in}} = \mathcal{V}(n_{\text{in}}), \quad v_{\text{out}} = \mathcal{V}(n_{\text{out}})$$

      Calculate arrive rate a: $a = \frac{v_{\text{out}}}{v_{\text{in}}} q_{k_t}$

      Update t_{in} and t_{out}

      if $t_{\text{in}} + \Delta n / q_{k_t} < \tau_{\text{out}}(k_t + 1)$ **then**

$$t_{\text{out}} = t_{\text{out}} + \frac{\Delta n}{a}, \quad t_{\text{in}} = t_{\text{in}} + \frac{\Delta n}{q_{k_t}}$$

      else

$$t_{\text{out}} = t_{\text{out}} + \frac{\left(\tau_{\text{out}}(k_t + 1) - t_{\text{in}}\right) q_{k_t}}{a}, \quad t_{\text{in}} = \tau_{\text{out}}(k_t + 1)$$

      end if

    until $t_{\text{in}} = \tau_{\text{in}}(k_t + 1)$

  end if

  Update: $\tau_{\text{out}}(k_t + 1) = t_{\text{out}}$, $Q_{\text{out}}(k_t + 1) = Q_{\text{out}}(k_t) + q_{k_t} \Delta t$

  Calculate travel time: $h_{k_t} = \tau_{\text{out}}(k_t + 1) - \tau_{\text{in}}(k_t + 1)$

end for

Algorithm 3 Flow propagation

Input: current entry time t_{in}, current exit time t_{out}, entry time $\tau_{\text{in}}(k)$ $(k = 1, 2, \cdots, N, N+1)$, cumulative inflow $Q_{\text{in}}(k)$ $(k = 1, 2, \cdots, N, N+1)$, exit time $\tau_{\text{out}}(k)$ $(k = 1, 2, \cdots, k_t)$, cumulative outflow $Q_{\text{out}}(k)$ $(k = 1, 2, \cdots, k_t)$,

Output: accumulative flow n_{in}, n_{out}

1: Calculate cumulative inflow $Q^{\text{in}}_{t_{\text{in}}}$ at time t_{in}

$$Q^{\text{in}}_{t_{\text{in}}} = \begin{cases} 0 & \text{if } t_{\text{in}} < \tau_{\text{in}}(1) \\ Q_{\text{in}}(s) + \frac{Q_{\text{in}}(s+1) - Q_{\text{in}}(s)}{\tau_{\text{in}}(s+1) - \tau_{\text{in}}(s)} \left(t_{\text{in}} - \tau_{\text{in}}(s)\right) & \text{if } \tau_{\text{in}}(s) \le t_{\text{in}} < \tau_{\text{in}}(s+1), s = 1, 2, \cdots, N \\ Q_{\text{in}}(N+1) & \text{if } t_{\text{in}} \ge \tau_{\text{in}}(N+1) \end{cases}$$

2: Calculate cumulative outflow $Q^{\text{in}}_{t_{\text{in}}}$ at time t_{in}

$$Q^{\text{out}}_{t_{\text{in}}} = \begin{cases} 0 & \text{if } t_{\text{in}} < \tau_{\text{out}}(1) \\ Q_{\text{out}}(s) + \frac{Q_{\text{out}}(s+1) - Q_{\text{out}}(s)}{\tau_{\text{out}}(s+1) - \tau_{\text{out}}(s)} \left(t_{\text{in}} - \tau_{\text{out}}(s)\right) & \text{if } \tau_{\text{out}}(s) \le t_{\text{in}} < \tau_{\text{out}}(s+1), s = 1, 2, \cdots, k_t \end{cases}$$

3: Calculate cumulative inflow $Q^{\text{in}}_{t_{\text{out}}}$ at time t_{out}

$$Q^{\text{in}}_{t_{\text{out}}} = \begin{cases} 0 & \text{if } t_{\text{out}} < \tau_{\text{in}}(1) \\ Q_{\text{in}}(s) + \frac{Q_{\text{in}}(s+1) - Q_{\text{in}}(s)}{\tau_{\text{in}}(s+1) - \tau_{\text{in}}(s)} \left(t_{\text{out}} - \tau_{\text{in}}(s)\right) & \text{if } \tau_{\text{in}}(s) \le t_{\text{out}} < \tau_{\text{in}}(s+1), s = 1, 2, \cdots, N \\ Q_{\text{in}}(N+1) & \text{if } t_{\text{out}} \ge \tau_{\text{in}}(N+1) \end{cases}$$

4: Calculate cumulative outflow $Q^{\text{in}}_{t_{\text{out}}}$ at time t_{out}

$$Q^{\text{out}}_{t_{\text{out}}} = \begin{cases} 0 & \text{if } t_{\text{out}} < \tau_{\text{out}}(1) \\ Q_{\text{out}}(s) + \frac{Q_{\text{out}}(s+1) - Q_{\text{out}}(s)}{\tau_{\text{out}}(s+1) - \tau_{\text{out}}(s)} \left(t_{\text{out}} - \tau_{\text{out}}(s)\right) & \text{if } \tau_{\text{out}}(s) \le t_{\text{out}} < \tau_{\text{out}}(s+1), s = 1, 2, \cdots, k_t \end{cases}$$

5: Calculate accumulative flow n_{in}, n_{out}

$$n_{\text{in}} = Q^{\text{in}}_{t_{\text{in}}} - Q^{\text{out}}_{t_{\text{in}}}$$
$$n_{\text{out}} = Q^{\text{in}}_{t_{\text{out}}} - Q^{\text{out}}_{t_{\text{out}}}$$